



# Ionic liquids with methotrexate moieties as a potential anticancer prodrug: Synthesis, characterization and solubility evaluation

Rahman Md. Moshikur<sup>a</sup>, Md. Raihan Chowdhury<sup>a</sup>, Rie Wakabayashi<sup>a,c</sup>, Yoshiro Tahara<sup>a</sup>, Muhammad Moniruzzaman<sup>b</sup>, Masahiro Goto<sup>a,c,\*</sup>

<sup>a</sup> Department of Applied Chemistry, Graduate School of Engineering, Kyushu University, 744 Motooka, Nishi-ku, Fukuoka 819-0395, Japan

<sup>b</sup> Chemical Engineering Department, Universiti Teknologi PETRONAS, 32610 Seri Iskandar, Perak, Malaysia

<sup>c</sup> Advanced Transdermal Drug Delivery System Center, Kyushu University, 744 Motooka, Nishi-ku, Fukuoka 819-0395, Japan

## ARTICLE INFO

### Article history:

Received 21 October 2018

Received in revised form 6 January 2019

Accepted 11 January 2019

Available online 14 January 2019

### Keywords:

Active pharmaceutical ingredient

Ionic liquid

Methotrexate

Solubility

Cytotoxicity

## ABSTRACT

The technological utility of active pharmaceutical ingredients (APIs) is enormously improved when they are converted into ionic liquids (ILs). API-ILs possess better aqueous solubility and thermal stability than that of solid-state salt or crystalline drugs. However, many such API-ILs are not biocompatible or biodegradable. In the current study, we synthesized a series of IL-APIs using methotrexate (MTX), a potential anticancer prodrug, and biocompatible IL-forming cations (choline and amino acid esters). The MTX-IL moieties were characterized through <sup>1</sup>H NMR, FTIR, p-XRD, DSC and thermogravimetric analysis. The solubility of the MTX-ILs was evaluated in simulated body fluids (phosphate-buffered saline, simulated gastric, and simulated intestinal fluids). An assessment of the in vitro antitumor activity of the MTX-ILs in a mammalian cell line (HeLa cells) was used to evaluate their cytotoxicity. The MTX-ILs showed aqueous solubility at least 5000 times higher than that of free MTX and two orders of magnitude higher compared with that of a sodium salt of MTX in both water and simulated body fluids. Importantly, a proline ethyl ester MTX prodrug showed similar solubility as the MTX sodium salt but it provided improved in vitro antitumor activity. These results clearly suggest that the newly synthesized API-ILs represent promising potential drug formulations.

© 2019 Elsevier B.V. All rights reserved.

## 1. Introduction

The development of smart drug delivery systems for anticancer drugs has been a challenging task for pharmaceutical researchers because of their polymorphisms, lower solubility and bioavailability [1–4]. Currently, new anticancer drugs are developed to achieve maximum therapeutic efficacy with minimal possible side-effects through oral or parenteral administration [3]. However, most chemotherapeutic agents exhibit undesirable physico-chemical properties such as low water solubility, low permeability (barriers to drug delivery), a narrow therapeutic window and a short half-life, along with systemic side-effects [5]. To avoid severe adverse effects, pharmaceutical scientists are trying to design drug delivery formulations specifically to kill tumor cells only, with little or no adverse effects on healthy tissues or cells. Methotrexate (MTX) is a biopharmaceutical classification systems class IV drug and has been approved by the USA Food and Drug Administration (FDA) as a chemotherapeutic agent. MTX possesses low permeability ( $C \log P = 0.53$ ), poor aqueous solubility (0.1 mg/mL) and

poor bioavailability (only 18% for doses >40 mg/m<sup>2</sup>) [6,7]. MTX is used clinically for the treatment of different types of cancer, rheumatoid arthritis, psoriasis, and other autoimmune diseases, and the induction of abortion (along with misoprostol) [6–9]. In general, MTX is absorbed by the gastrointestinal tract (GIT). The rate of absorption mainly depends on the drug dose [10]. For example, the therapeutic and toxic plasma concentration of MTX varies from low-dose therapy (0.005 and 0.001 µg/mL, respectively) to high-dose therapy (2.27 and 4.54 µg/mL, respectively) [11]. On the basis of this erratic GIT absorption, it has been suggested that high-dose therapy (>25 mg) should be administered orally or parenterally [7]. Although MTX tablets and injections were FDA approved in 1980, high-dose oral therapy could increase the risk of adverse effects, such as GI toxicity [12,13], because of poor MTX solubility and bioavailability [7]. The therapeutic effect of MTX is largely influenced by its low tumor cell uptake and therapeutic doses can cause severe side effects such as diarrhea and ulcerative stomatitis [13].

To address these limitations, an ionic liquid (IL) formulation of active pharmaceutical ingredients (APIs), such as MTX, is a promising technique to deliver drugs. Recently, ILs have been used extensively to form IL-API because they provide many advantages over solid or crystalline forms of drugs [14–16]. IL-APIs can also address the issue of polymorphisms, a significant problem in drug delivery. The combination of poorly water-

\* Corresponding author at: Department of Applied Chemistry, Graduate School of Engineering, Kyushu University, 744 Motooka, Nishi-ku, Fukuoka 819-0395, Japan.

E-mail address: [m-goto@mail.cstm.kyushu-u.ac.jp](mailto:m-goto@mail.cstm.kyushu-u.ac.jp) (M. Goto).

soluble APIs with specific counter-ions is an excellent approach to upgrade conventional pharmaceuticals using an IL-based strategy [16]. This prodrug technique can eliminate the effect of drug polymorphisms or crystallinity, which is often responsible for reducing therapeutic efficiency, bioavailability and thermal stability [15–17]. Recently, Rogers groups demonstrated the successful application of an IL formulation to deliver the poorly soluble drug sulfasalazine and reported that solubility increased 4000 times and bioavailability was 2.5-fold higher compared with that of free drug [18]. Yoshiura et al. [19] described an IL-based microemulsion for the delivery of MTX and demonstrated that MTX penetration through pig skin increased dramatically. Moniruzzaman et al. [20] reported a novel imidazolium-based IL-in-oil microemulsion, in which MTX dissolved more efficiently than in water. However, an MTX-based API-IL, either as an anion or as a cation, has not previously been reported.

In the present study, we explored the use of the IL-API approach to solve the deficiencies of the solid drug MTX, by creating an MTX anion-based IL, and report the synthesis, characterization, solubility (both in aqueous and physiological fluids) and *in vitro* antitumor activity of the MTX-IL moieties.

## 2. Experimental

### 2.1. Materials and methods

MTX (anhydrous, >98% purity) was purchased from Wako Chemicals Ltd. (Osaka, Japan). L-Proline, L-aspartic acid, tetramethylammonium hydroxide (15% in water), and tetrabutylphosphonium hydroxide (40% in water) were obtained from Wako Chemicals Ltd. (Osaka, Japan). L-Phenylalanine with a high level of purity (>98.0%) was purchased from Kishida Chemical Co. Ltd. (Osaka, Japan), and 1-ethyl-3-methylimidazolium chloride was purchased from TCI America (Tokyo, Japan). The concentrations of ammonium, phosphonium, choline and imidazolium were determined via titration. All other reagents, solvents and materials were of analytical grade and were used without any further purification.

Gibco minimum essential media (MEM), Opti-MEM, fetal bovine serum, and antibiotic-antimycotic were purchased from Thermo Fisher Scientific (Waltham, MA, USA). Dulbecco's phosphate buffered saline (PBS) and 0.25% trypsin/1 mM ethylenediaminetetraacetic acid were obtained from Nacalai Tesque (Kyoto, Japan). A WST-8 (2-(2-methoxy-4-nitrophenyl)-3-(4-nitrophenyl)-5-(2,4-disulfophenyl)-2H-tetrazolium monosodium salt) cell counting kit was obtained from Dojindo Molecular Technologies, Inc. (Kumamoto, Japan). The HeLa cell line was provided by the RIKEN cell bank (Tsukuba, Japan).

### 2.2. General synthetic procedure for cations and MTX-IL moieties

The desired cations were synthesized in accordance with our previously reported procedure [2,21]. The synthetic route for the preparation of amino acid esters (AAEs) is outlined in Scheme S1 and involves a reaction between amino acids and thionyl chloride (mole ratio of thionyl chloride: amino acid = 1.5:1) in ethanol and neutralization using an ammonium solution (two equivalents) as a base [2]. The synthetic route for the other cations outlined in scheme S2 involves adding an equimolar amount of silver oxide to the respective chloride salt of the cations [21]. Finally, MTX anion-containing IL-API moieties were synthesized as shown in Scheme S3, through the ionization of a hydrophobic MTX hydrate and hydroxide salts of the desired cations in methanol at 40 °C for 2 h (see supporting information for details).

### 2.3. NMR measurements

The <sup>1</sup>H NMR spectra were recorded using a JEOL ECZ400S 400 MHz spectrometer (Tokyo, Japan) in deuterated dimethyl sulfoxide (2.5 ppm)/ methanol (3.3 ppm). The NMR solvents were obtained

from Wako Pure Chemical Industries Ltd. The coupling constants (*J*) are reported in Hertz (Hz). The DeltaV software package (version 5.0.5.1, JEOL) was used to process the spectra. The purities of the synthesized MTX-IL moieties were determined using the following equation:

$$\text{Purity (\%)} = \left[ \frac{\sum I(\text{product})}{\sum I(\text{total})} \right] \times 100 \quad (1)$$

where, *I* represents the relative area of each signal [22].

### 2.4. Fourier transform infrared analysis

The Fourier transform infrared (FT-IR) spectra of the MTX-ILs were recorded using a Perkin Elmer spectrometer (Frontier FT/IR, Waltham, MA) in the range 400–4000 cm<sup>-1</sup> with an accumulation of 20 scans.

### 2.5. Thermogravimetric analysis

Thermogravimetric and derivative thermogravimetric analysis (TGA/DTG) was performed using a Hitachi High-Technologies TG/DTA 7300 (Tokyo, Japan) under a flow of nitrogen. Samples weighing approximately 10 to 20 mg were analyzed in an aluminum crucible and were heated from 30 to 550 °C using a constant heating rate of 5 °C min<sup>-1</sup> with a 30 min isothermal step at 70 °C.

### 2.6. Differential scanning calorimetry

Differential scanning calorimetric (DSC) measurements were carried out using a Hitachi High-Technologies DSC X7000 (Tokyo, Japan) to characterize the thermal behavior of the drug moieties. Standard aluminum pans containing 4 to 6 mg samples were crimped with an aluminum lid using a press (T Zero sample press), and heated from –50 to 300 °C at a rate of 10 °C min<sup>-1</sup> under constant nitrogen at 30 mL/min. An empty pan, sealed in the same way as the sample, was used as a reference.

### 2.7. Powder X-ray diffraction (p-XRD)

For structural analysis, p-XRD analyses were performed using a high-resolution X-ray diffractometer (Rigaku, Smartlab 9 kW, Tokyo, Japan) with monochromatized and Ni-filtered Cu K $\alpha$  radiation ( $\lambda$  = 1.5418 Å), operating at 40 kV and 30 mA. The data were collected using the 2 $\theta$  range of 5–50° with a scanning speed of 2°/min with 0.02°.

### 2.8. Partitioning coefficient determination

Approximately 2 to 3 mg of free MTX-ILs were added to a mixture of 5 mL of Milli-Q-water and 5 mL of octanol. The mixtures were allowed to mix overnight at room temperature with constant shaking in the dark. Then, the solution was centrifuged at 10,000g for 60 min to separate the layers. The concentration of free MTX in each layer was quantified through UV spectroscopy (JASCO V-750, Japan) using known concentrations of a standard at 302 nm. The partition coefficient, log *P*<sub>o/w</sub>, was determined using the following equation:

$$\log P_{o/w} = \log \left( \frac{\text{Solute}_{\text{octanol}}}{\text{Solute}_{\text{water}}} \right) \quad (2)$$

where, Solute<sub>octanol</sub> and Solute<sub>water</sub> represent the amount of free MTX in octanol and water, respectively.

### 2.9. Media for solubility studies

Milli-Q-water, PBS, simulated intestinal fluid (SIF) and simulated gastric fluid (SGF) were used as dissolution media to perform a solubility study of the MTX-IL moieties. PBS (pH = 7.4) was purchased from Nacalai Tesque Inc. (Kyoto, Japan). SIF (pH = 6.8, without pancreatic enzyme) and SGF (pH = 1.2, without pepsin enzyme) were prepared

following United States Pharmacopeia guidelines. Briefly, SIF buffer was prepared by dissolving 0.0896 g of NaOH and 0.6805 g of  $\text{KH}_2\text{PO}_4$  in 100 mL of water in a volumetric flask. SGF was prepared by dissolving 0.200 g of NaCl and 0.7 mL of concentrated HCl (to adjust the pH to 1.2) in a 100 mL volumetric flask and diluting the solution using water.

### 2.10. Solubility of the MTX-IL moieties

To determine the aqueous solubility of the MTX-IL moieties, equilibrium solubility was determined using a “shake-flask” method. Briefly, an excess amount of MTX-ILs was mixed in 0.5 mL of water or physiological fluids (PBS, SIF, or SFG), and the mixtures were stirred thoroughly for 24 h at 20 °C. Then, each solution was centrifuged at 10,000g for 60 min to separate the solid-liquid phases. The liquid phase was filtered using a 0.2  $\mu\text{m}$  syringe filter to remove the remaining solid particles. The filtrate was analyzed using UV-vis spectroscopy, with quartz cells at a wavelength of 302 nm, which is the wavelength of the maximum absorbance of MTX. Duplicate samples were measured. A predetermined calibration curve was used to determine the amount of drug in the dissolution media (for all curves  $R^2 > 0.9957$ ), which was constructed using different solutions with known concentrations of the corresponding MTX-ILs.

### 2.11. In vitro antitumor activity

To evaluate the antitumor activity of the MTX-ILs and sodium salt of MTX, a WST cell viability assay was conducted using the HeLa mammalian cell line, as described in the literature [2]. Briefly, the cells were cultured in MEM containing 10% fetal bovine serum and 1% antibiotic-antimycotic. The cells were seeded into 96-well flat-bottomed plates at 5000 cells/well and, then incubated for 24 h at 37 °C under a 5%  $\text{CO}_2$  atmosphere. Samples were prepared in Opti-MEM at varying concentrations in the range 0.01–50 mM. A total of 100  $\mu\text{L}$  of each sample solution was replaced in each well, and the plates were incubated for 24 h. After incubation, the solution was removed through washing

with PBS and 100  $\mu\text{L}$  of the WST cell counting kit solution in Opti-MEM was added to each well to measure the mitochondrial activity of the cells. After a further 3 h incubation at 37 °C in a  $\text{CO}_2$  incubator, the absorbance of the supernatant ( $A_{\text{treated}}$ ) was measured at 450 nm using a microplate spectrophotometer (Bio-Rad, Tokyo, Japan). The cell viability compared with untreated cells ( $A_{\text{control}}$ ) was calculated using the following equation:

$$\text{Cell viability (\%)} = (A_{\text{treated}}/A_{\text{control}}) \times 100 \quad (3)$$

All tests were performed in triplicate and the average values are reported. Microsoft Excel 2016 (Microsoft, Washington, USA) was used to perform the statistical analysis. Data are presented as the mean with the standard deviation.

### 2.12. Statistical analysis

Statistical analysis was performed using GraphPad Prism version 6 software (GraphPad Software, Inc., La Jolla, CA). Statistical significance was evaluated through a one-way analysis of variance (ANOVA) followed by Tukey's post-hoc test for multiple comparisons.

## 3. Results and discussion

### 3.1. Synthesis and characterization of MTX-IL moieties

API-IL prodrugs represent a highly promising approach to turn crystalline drugs into a liquid form to improve their physicochemical or biological activity. To synthesize IL-APIs (Fig. 1B), the hydrophobic crystalline drug MTX is considered an anion which possesses two acidic protons ( $\text{pK}_a = 2.9$  and 4.6) and a nitrogen basic site ( $\text{pK}_a = 6.6$ ) in its structure [23].

Several types of cation, such as AAE, cholinium, imidazolium, quaternary ammonium and quaternary phosphonium, are described in Fig. 1A. They reportedly have low toxicities or additional biological activity

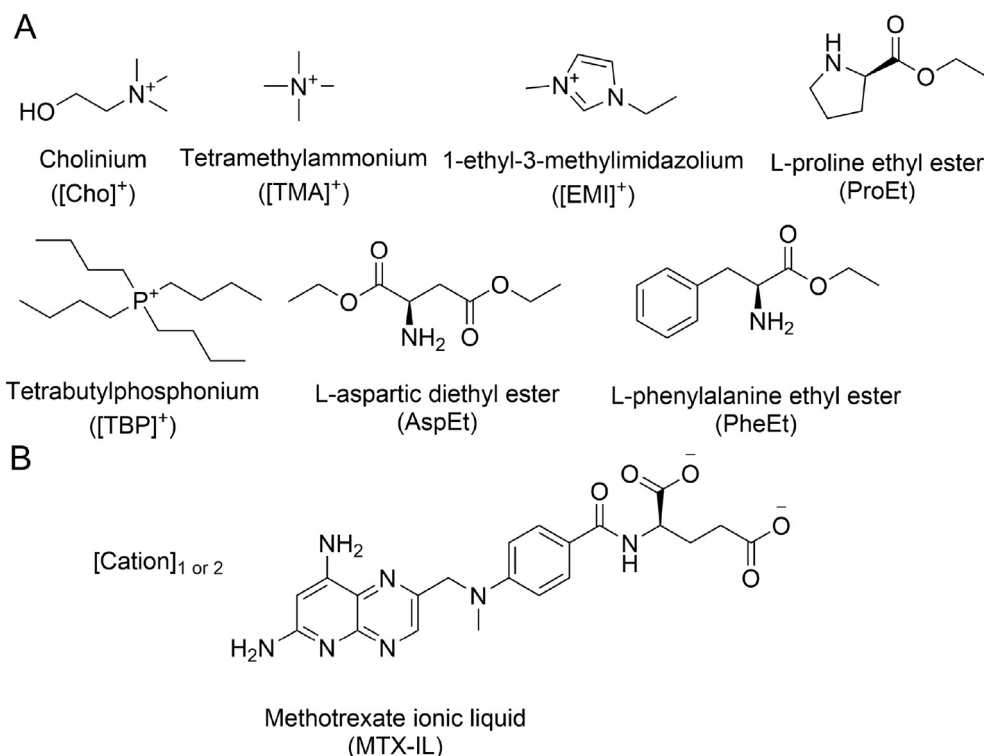


Fig. 1. Structures, names, and abbreviations for the (A) IL-forming cations and (B) MTX-ILs used in this study.

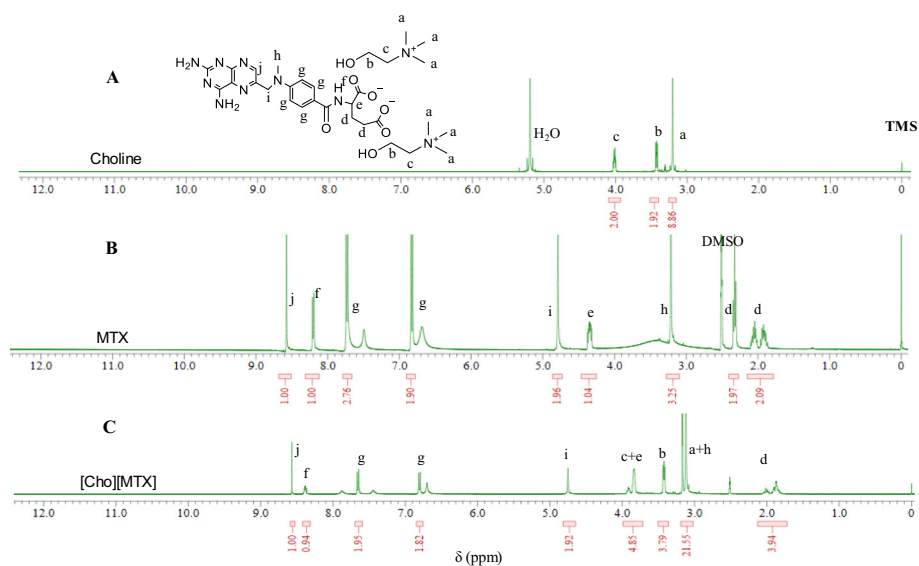


Fig. 2. <sup>1</sup>H NMR spectra of (A) the Cho cation, (B) free MTX and (C) [Cho][MTX].

among their corresponding groups, and they were chosen as a counterion for use during MTX-IL moiety synthesis [2,24–28]. The rationale for the choice of these cations is their potential to improve aqueous solubility and skin permeability when combined with free drugs [18]. However, MTX anion-containing IL-API moieties were synthesized through ionization of hydrophobic hydrate MTX and AAEs or hydroxide salts of the desired cations in methanol. The results of the <sup>1</sup>H NMR spectroscopy analysis show that the stoichiometry between the two constituents for the [Cho][MTX] compounds was 1:2 (Fig. 2). In the case of the MTX-AAEs, the stoichiometry ratio was 1:1 because of the lower pK<sub>b</sub> value of AAE cations (the pK<sub>b</sub> value of AspEt is 6.6) (Fig. S19–S21). However, all the MTX-IL moieties demonstrated high yields and were present as solids except [Cho][MTX], [EMi][MTX] and [TBP][MTX] (Table S1). The purities of all the synthetic compounds determined using <sup>1</sup>H NMR were ≥ 97.0% (Table S1).

While the stoichiometry ratio of the MTX-ILs was assessed using <sup>1</sup>H NMR, the assessment of fully ionization of the moieties was performed using FT-IR. FT-IR measurements were performed to further understand the interaction between MTX and the cations and then compare the moieties with a fully ionized sodium salt of MTX. In the FT-IR spectrum of free MTX, characteristic peaks were observed at 1678 cm<sup>-1</sup>, 1640 cm<sup>-1</sup> and 1606 cm<sup>-1</sup> for C=O stretching of the –COOH groups,

C=C stretching of the MTX benzene ring and the MTX amide, respectively. The spectrum of the [ProEt][MTX] moieties was confirmed to contain characteristic peaks at 1616 cm<sup>-1</sup> and 1590 cm<sup>-1</sup> for C=C stretching of the MTX benzene ring and MTX amide, respectively (Fig. 3). These peaks were also observed in the [Na][MTX] spectrum. Characteristic peaks for C=O stretching of the –COOR groups of ProEt were observed at nearly 1731 cm<sup>-1</sup> and this shifted to ca. 1726 cm<sup>-1</sup> in the ProEt cation [2]. The characteristic peaks for C–H stretching of the ethyl group were observed at ca. 2981 cm<sup>-1</sup> in the [ProEt][MTX] spectrum and were attributed to the ethyl group of ProEt. Similarly, characteristic peaks for other cations were observed in their respective MTX-IL spectra. For all spectra of the MTX-IL moieties, the characteristic peaks for C=O stretching of –COOH groups at 1678 cm<sup>-1</sup>, as seen in free MTX, were not observed (Figs. S1–S3). However, a new weak shoulder peak appeared at ca. 1602 cm<sup>-1</sup>, which has been attributed to hydrogen bonding between carbonyl groups and respective cations (i.e. amine/ammonium/phosphonium groups of cations). These similar weak shoulder peaks were observed at 1602 cm<sup>-1</sup> in the [Na][MTX] spectrum (Fig. 3).

The amorphous structure of API-ILs is the important parameter to achieve maximum therapeutic efficacy. It has been reported that amorphous APIs have higher solubility, higher dissolution rate and reduced

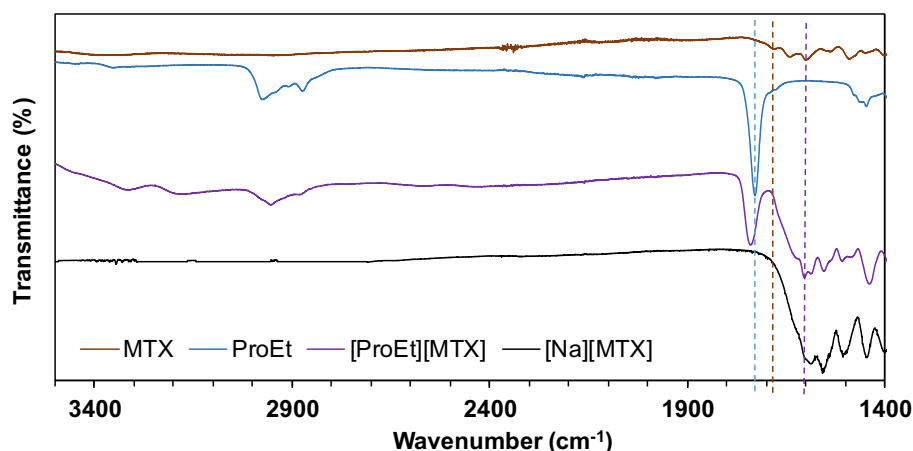


Fig. 3. FT-IR spectra of free MTX, ProEt, [ProEt][MTX] and [Na][MTX].

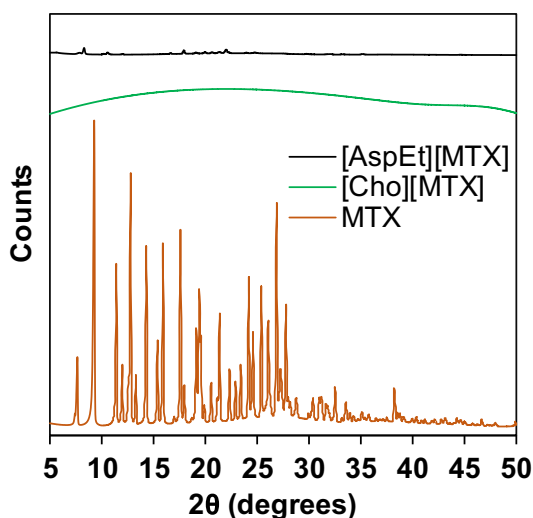


Fig. 4. The XRD spectra of [AspEt][MTX], [Cho][MTX] and free MTX.

polymorphism than corresponding crystals [29]. It reveals a great ability to stick together during tableting and reduce the amount of additives, which simplify the formulation procedure [30]. The XRD pattern shown in Fig. 4 confirmed the amorphous phase of the MTX-ILs while the free MTX was crystalline in nature. Several characteristic sharp peaks were observed in the X-ray diffractogram of free MTX between the  $2\theta$  of  $5^\circ$  and  $30^\circ$ . The most promising peaks of MTX were identified at 9.3, 11.4, 12.8, 14.3, 15.9, 17.6, 19.4, 21.4, 24.2, 25.4, 26.9 and 27.8 ( $2\theta$  scattered angles), which clearly indicated the crystalline nature of the free MTX [31]. All sharp crystalline peaks were diffused in the diffractogram of the MTX-ILs, as shown in Fig. 4, which is indicative of the amorphous nature of the MTX-IL moieties. Therefore, these results indicate that free MTX was encapsulated or homogeneously distributed in the cationic matrix and then dispersed molecularly (Fig. S4).

### 3.2. Thermophysical studies of MTX-IL moieties

The thermal behavior of all synthetic MTX-IL compounds was investigated using thermoanalytic methods, as well as DSC, TGA and DTG, to provide evidence on the possible thermal interaction between free drug and various cations. Initially, we evaluated the thermal stabilities of the synthesized MTX-IL moieties through TGA and measured the onset ( $T_{5\%onset}$ ) temperatures (Table 1 and Fig. 5). The MTX-ILs showed similar or lower thermal stabilities than that of the free hydrate MTX (Table 1). In the TGA and DTG thermograms of free MTX and [Cho][MTX], the free hydrate MTX thermogram showed a three step decomposition with 37.26% loss of its initial mass on heating to  $550^\circ\text{C}$ , which was clearly seen in the DTG thermogram. The first decomposition step occurred from  $40^\circ\text{C}$  to  $75^\circ\text{C}$ , and was attributed to removal of volatile

Table 1  
Physicochemical properties of the free hydrate MTX and MTX-IL moieties.

| Compound     | Log P <sub>o/w</sub> | DSC                 |                     | TGA                       |
|--------------|----------------------|---------------------|---------------------|---------------------------|
|              |                      | T <sub>g</sub> (°C) | T <sub>m</sub> (°C) | T <sub>5%onset</sub> (°C) |
| Methotrexate | -1.98                | 114                 | 154                 | 246                       |
| [Cho][MTX]   | -3.62                | 27                  | 143                 | 200                       |
| [TMA][MTX]   | -3.99                | 46                  | 141                 | 208                       |
| [EMI][MTX]   | -3.83                | 45                  | 112                 | 251                       |
| [TBP][MTX]   | -1.17                | 17                  | 137                 | 296                       |
| [ProEt][MTX] | -2.82                | 93                  | 120                 | 171                       |
| [AspEt][MTX] | -2.56                | 104                 | 164                 | 142                       |
| [PheEt][MTX] | -1.91                | 103                 | 142                 | 175                       |

materials and surface adsorbed water molecules with a ca. 8% loss of mass. The second decomposition step corresponds to a 2% dehydration of drug from  $75^\circ\text{C}$  to  $120^\circ\text{C}$ , which is required to remove structural water. This value of mass loss is in good agreement with the theoretical percentage of water contained in the free drug (ca. 10%). After the removal of the water, anhydrous MTX is formed and shows good thermal stability in a  $120$ – $228^\circ\text{C}$  temperature range. The actual thermal decomposition of free anhydrous MTX takes place from  $232^\circ\text{C}$  to  $550^\circ\text{C}$  with a mass loss of ca. 52.7% of its initial mass. The  $T_{5\%onset}$  of the free hydrate MTX is approximately  $246^\circ\text{C}$ . These results are in agreement with previous findings [32].

The MTX-IL moieties exhibited slightly different results compared with the free hydrate MTX. For example, [Cho][MTX] demonstrated three main thermal phenomena. The first and second weight losses of 3.72% and 1% at  $30$ – $75^\circ\text{C}$  and  $75$ – $150^\circ\text{C}$ , respectively, were attributed to the removal of volatile materials and surface adsorbed water, and structural water molecules. Similar decomposition steps were also found for all MTX-IL moieties (Fig. S5). It was found that the MTX-IL moieties demonstrated good thermal stability up to  $200^\circ\text{C}$  except [AAEs][MTX]. The  $T_{5\%onset}$  temperatures of decomposition for the MTX-IL moieties are shown in Table 1.

To further investigate the physical properties such as the melting points and/or phase transitions of the MTX-ILs, we carried out DSC analyses. The DSC thermograms are shown in Fig. 6. The free MTX exhibited a characteristic sharp endothermic peak at  $154^\circ\text{C}$  with an enthalpy of relaxation of 8 mW, which corresponds to its melting point. It has been reported that the thermogram of choline exhibits no endothermic peak during the complete heating procedure ( $20^\circ\text{C}$ – $300^\circ\text{C}$ ) [33]. However, in the thermogram of [Cho][MTX] the characteristic sharp endothermic peak shifted to  $143^\circ\text{C}$ , which is an indication of a significant change in the physical state from crystalline to amorphous.

Similarly, IL moieties of MTX with different cations ([ProEt][MTX]) showed variable characteristic sharp endothermic peaks at different temperatures without any phase transformation (Fig. 6 and Fig. S6–S8). These results confirmed that there was a strong physicochemical interaction between free drug and cations.

### 3.3. Solubility study of the MTX-IL moieties

Solubility and bioavailability of a drug molecule is essential physicochemical parameters in order to predict their mode of release mechanisms and possible in vivo behavior into the human body. The pharmacokinetic and pharmacodynamics parameters of drug molecules were limited due to their insufficient aqueous solubility and permeability in the simulated body fluids following oral administration. To determine if we had achieved our goal of increased solubility, we carried out an equilibrium solubility analysis (undissolved solid MTX-IL remains in equilibrium within a saturated aqueous solution) of MTX-ILs in various physiological fluids at room temperature and atmospheric pressure. All MTX-IL compounds showed higher solubility than free MTX in both water (Fig. S9) and buffers (Fig. 7). As expected, [Cho][MTX] showed higher aqueous solubility than the other MTX-ILs, and this was 5280 times higher than that of free MTX (0.15 mg/mL) or two times higher than that of an MTX sodium salt in PBS (pH = 7.4). The presence of hydroxyl groups in the alkyl chains of the cholinium cation, which enhance the hydrogen bonding capacity and polarity of a cation, increases its aqueous solubility. These results are similar to previously reported data, in which choline-based drugs showed higher aqueous solubility than free drugs. For example, choline naproxen and choline tolmetin showed a 6700- and 8000-fold higher aqueous solubility than their corresponding free drugs, respectively [34].

The aqueous solubility of MTX-ILs in PBS decreases in accordance with the following sequence: [PheEt][MTX] < [AspEt][MTX] < [ProEt][MTX] < [TBP][MTX] < [EMI][MTX] < [TMA][MTX] < [Cho][MTX]. This depends on the chemical structure of cations such as ammonium, imidazolium, phosphonium, choline and AAEs (Fig. 7). Table 1 shows

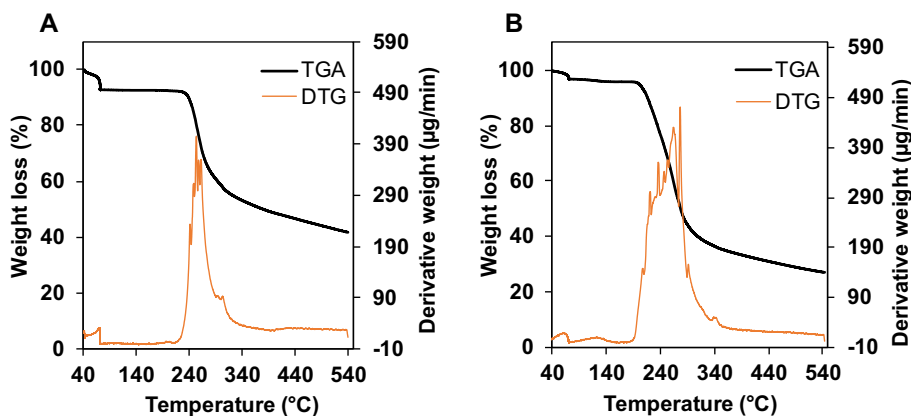


Fig. 5. TGA and DTG thermograms of (A) free hydrate MTX and (B) [Cho][MTX] measured in a nitrogen atmosphere with a heating rate of  $10\text{ }^{\circ}\text{C min}^{-1}$ .

the Log  $P$  of the MTX-ILs. [Cho][MTX] (Log  $P = -3.62$ ) showed the highest solubility in PBS among the MTX-ILs, free MTX and an MTX sodium salt, because of its high hydrophilicity. The relative aqueous solubility of the MTX-ILs mainly depends on the hydrophilicity of the cations. However, although the hydrophilicity of [ProEt][MTX] (Log  $P = -2.82$ ) is higher than that of [TBP][MTX] (Log  $P = -1.17$ ), the aqueous solubility of [ProEt][MTX] is lower than that of [TBP][MTX], yet that of both MTX-ILs is higher than that of free MTX.

Next, we evaluated the solubility of the MTX-ILs in different simulated physiological body fluids such as SGF (pH 1.2), and SIF (pH 6.8). The solubility of the MTX-ILs was much higher compared with that of free MTX in all physiological media. In SGF, [Cho][MTX] showed the highest solubility because of an increase in the hydrophilicity of the cholinium cation produced by the presence of hydrophilic hydroxyl groups in the alkyl chains. However, [TMA][MTX] showed a slightly higher solubility than [Cho][MTX] in SIF, because of its high hydrophilicity at neutral pH. The solubility of [TMA][MTX] in PBS or SGF was lower than that of [Cho][MTX] because of the effect of the low pH and ionic strength of the testing media. In all cases, [PheEt][MTX] showed the lowest solubility in water and the three simulated body fluids (PBS, SGF and SIF). The PheEt cation increased the hydrophobicity of the MTX-ILs because of the presence of a hydrophobic benzene ring in its side chains.

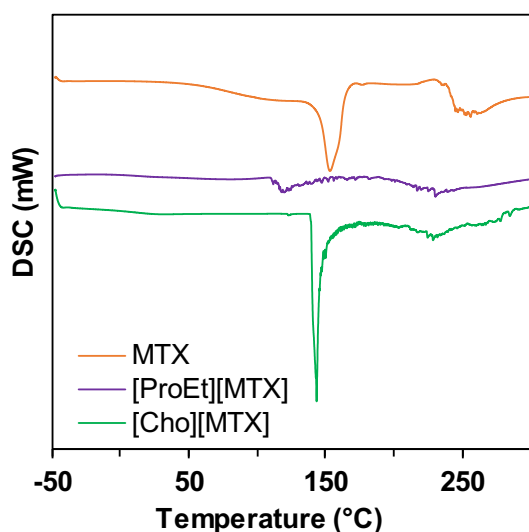


Fig. 6. DSC thermograms of free MTX, [ProEt][MTX] and [Cho][MTX].

### 3.4. *In vitro* antitumor activity of the MTX-ILs

Finally, the *in vitro* antitumor activity of the MTX-ILs was evaluated using a HeLa mammalian cancer cell line, and compared with that of MTX sodium salt. Before comparing the antitumor activity of the MTX-IL moieties, we evaluated the cytotoxicity of the cations (Fig. 8A). Among the cations, TBP showed the lowest  $\text{IC}_{50}$  because of the presence of a long alkyl chain in the cation. In the AAEs, the high cytotoxicity of PheEt could be attributed to a strong  $\pi$ - $\pi$  interaction between the cation and the cell membrane, leading to a rapid disruption of the cell structure. ProEt showed lower toxicity than the other cations because of the presence of a cyclic secondary amine in its structure [2]. Both ProEt and AspEt demonstrated relatively low toxicity because of their higher hydrophilicity (Table 1).

The *in vitro* antitumor activity of the MTX-ILs mainly depends on the toxic nature of the relevant cations (Fig. 8B). Among all the MTX-IL moieties, [TBP][MTX] was the most toxic in HeLa cells because of the presence of a highly cytotoxic cation (Fig. 8A), which enhanced the penetration of MTX into the cell membrane and disrupted its physiological functions, ultimately leading to cell death. A similar result was obtained in [PheEt][MTX] and [EMI][MTX] because of the presence of a benzene or pyridine ring, which is attributed to a strong  $\pi$ - $\pi$  interaction between the hydrophobic or lipophilic cations and the plasma membrane of

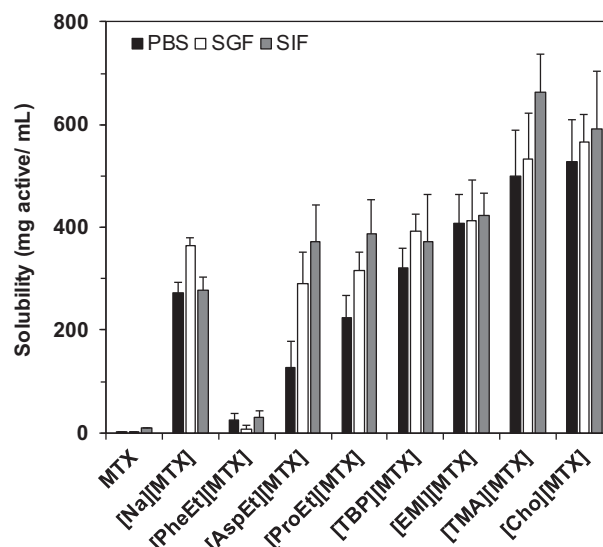
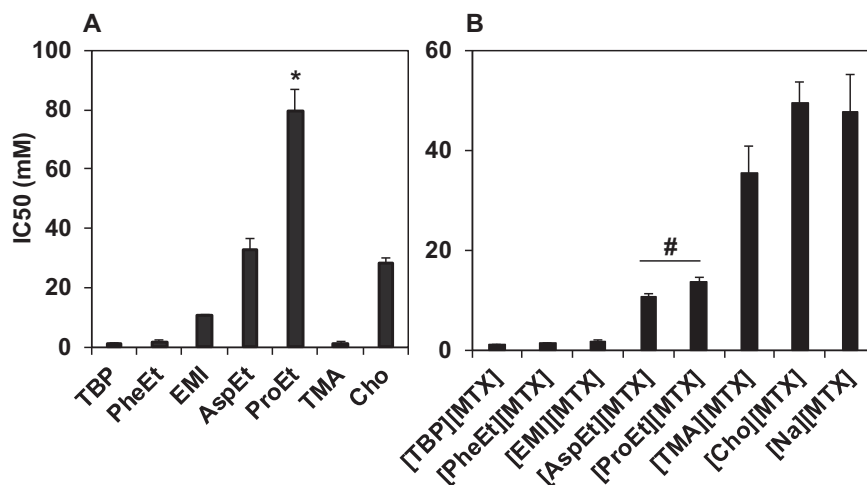


Fig. 7. Solubility of MTX-IL moieties in buffers (SIF, SGF and PBS).



**Fig. 8.** In vitro antitumor activity of MTX-IL moieties in HeLa cells. Effect of (A) cations derived from IL-forming cationic salts, and (B) MTX-IL moieties. Statistical significance was evaluated by one-way ANOVA followed by Tukey's post-hoc test for multiple comparisons. \* $P < 0.05$  versus all the other cations, # $P < 0.05$  versus all the other MTX-ILs. Data are expressed as mean  $\pm$  SD,  $n = 3$ .

cells, leading to rapid disruption of the cell structure. These results are in agreement with published work showing that higher hydrophobicity or long alkyl chains leads to high toxicity [1,2].

Ammonium-based IL moieties such as [TMA][MTX] and [Cho][MTX] showed the least toxicity whereas the AAE- and imidazolium-based MTX-ILs showed relatively high antitumor activity. These cations could be partially attributed to their high aqueous solubility and partition coefficient (Table 1), which reduced their interaction with the lipid bilayer of the cell membrane. The higher hydrophilicity of MTX-ILs could reduce the penetration of MTX through cell membrane by decreasing the lipophilicity of the IL form. Interestingly, the ProEt and AspEt cations were not toxic when administered alone (Fig. 8A). However, the AAE-based MTX-ILs with low toxicity ([ProEt][MTX] and [AspEt][MTX]) showed enhanced toxicity compared with a sodium salt of MTX because of their lower hydrophilicity. The ProEt cation-based MTX-IL showed lower toxicity than either the AspEt or PheEt cation-based MTX-IL because of the higher hydrophilicity of [ProEt][MTX] (Table 1). Therefore, the enhanced cytotoxic activity in a cancer cell line of these cations compared with their sodium analogs can be related to their greater lipophilicity.

#### 4. Conclusions

The current study reported a new series of IL-APIs consisting of MTX as an anion and biocompatible ILs, such as choline and AAEs, as a cation. Characterization studies (including NMR, FTIR, DSC and TGA) showed the successful synthesis of IL-MTX APIs with excellent API properties. The solubility of the MTX-IL moieties in simulated body fluids improved significantly compared with MTX and MTX sodium salts. Importantly, the prodrugs [AspEt][MTX] and [ProEt][MTX] showed enhanced in vitro antitumor activity compared with that of MTX sodium salt. The results reported here could play a significant role in the development of MTX-IL-assisted drug delivery systems that take advantage of the various attractive properties of ILs.

#### Acknowledgments

This work was supported by a Grant-in-Aid for Scientific Research (S) JP16H06369 from the Ministry of Education, Culture, Sports, Science and Technology of Japan. R.M.M thanks the Government of Japan (MEXT, Japan) for providing a scholarship. The authors also thank Dr. M. Watanabe for facility support for NMR, TGA, DSC and XRD. We thank Conn Hastings, PhD, from Edanz Group ([www.edanzediting.com/ac](http://www.edanzediting.com/ac)) for editing a draft of this manuscript.

#### Declaration of interests

None.

#### Appendix A. Supplementary data

Supplementary data to this article can be found online at <https://doi.org/10.1016/j.molliq.2019.01.063>.

#### References

- A.M.O. Azevedo, S.P.F. Costa, A.F.V. Dias, A.H.O. Marques, P.C.A.G. Pinto, K. Bica, A.K. Ressmann, M.L.C. Passos, A.R.T.S. Araújo, S. Reis, M.L.M.F.S. Saraiva, Anti-inflammatory choline based ionic liquids: insights into their lipophilicity, solubility and toxicity parameters, *J. Mol. Liq.* 232 (2017) 20–26, <https://doi.org/10.1016/j.molliq.2017.02.027>.
- R.M. Moshikur, M.R. Chowdhury, R. Wakabayashi, Y. Tahara, M. Moniruzzaman, M. Goto, Characterization and cytotoxicity evaluation of biocompatible amino acid esters used to convert salicylic acid into ionic liquids, *Int. J. Pharm.* 546 (2018) 31–38, <https://doi.org/10.1016/j.ijpharm.2018.05.021>.
- S. Kalepu, V. Nekkanti, Insoluble drug delivery strategies: review of recent advances and business prospects, *Acta Pharm. Sin. B* 5 (2015) 442–453, <https://doi.org/10.1016/j.apsb.2015.07.003>.
- M. Lotfi, M. Moniruzzaman, M. Sivapragasam, S. Kandasamy, M.I. Abdul Mutalib, N.B. Alitheen, M. Goto, Solubility of acyclovir in nontoxic and biodegradable ionic liquids: COSMO-RS prediction and experimental verification, *J. Mol. Liq.* 243 (2017) 124–131, <https://doi.org/10.1016/j.molliq.2017.08.020>.
- I. Ali, M.N. Lone, Z.A. Allothman, A. Alwarthan, Insights into the pharmacology of new heterocycles embedded with oxopyrrolidine rings: DNA binding, molecular docking, and anticancer studies, *J. Mol. Liq.* 234 (2017) 391–402, <https://doi.org/10.1016/j.molliq.2017.03.112>.
- J. Chen, L. Huang, H. Lai, C. Lu, M. Fang, Q. Zhang, X. Luo, Methotrexate-loaded PEGylated chitosan nanoparticles: synthesis, characterization, and in vitro and in vivo antitumor activity, *Mol. Pharm.* 11 (2014) 2213–2223, <https://doi.org/10.1021/mp400269z>.
- Z.A. Khan, R. Tripathi, B. Mishra, Methotrexate: a detailed review on drug delivery and clinical aspects, *Expert Opin. Drug Deliv.* 9 (2012) 151–169, <https://doi.org/10.1517/17425247.2012.642362>.
- R. Tondwal, M. Singh, Effect of increasing alkyl chain of 1st tier dendrimers on binding and release activities of methotrexate drug: an in vitro study, *J. Mol. Liq.* 211 (2015) 466–475, <https://doi.org/10.1016/j.molliq.2015.07.033>.
- F. Yang, N. Kamiya, M. Goto, Transdermal delivery of the anti-rheumatic agent methotrexate using a solid-in-oil nanocarrier, *Eur. J. Pharm. Biopharm.* 82 (2012) 158–163, <https://doi.org/10.1016/j.ejpb.2012.05.016>.
- R.M. Bremnes, L. Slørdal, J. Aarbakke, E. Wist, Dose-dependent pharmacokinetics of methotrexate and 7-hydroxymethotrexate in the rat in vivo, *Cancer Res.* 49 (1989) 6359–6364 (doi:2804982).
- R. Regenthal, M. Krueger, C. Koepfel, R. Preiss, Drug levels: therapeutic and toxic serum/plasma concentrations of common drugs, *J. Clin. Monit. Comput.* 15 (1999) 529–544, <https://doi.org/10.1023/A:1009935116877>.
- C.Z. Yang, C.Y. Liang, D. Zhang, Y.J. Hu, Deciphering the interaction of methotrexate with DNA: spectroscopic and molecular docking study, *J. Mol. Liq.* 248 (2017) 1–6, <https://doi.org/10.1016/j.molliq.2017.10.017>.

- [13] D.J. Chatterjee, W.Y. Li, R.T. Koda, Effect of vehicles and penetration enhancers on the in vitro and in vivo percutaneous absorption of methotrexate and edatrexate through hairless mouse skin, *Pharm. Res.* 14 (1997) 1058–1065, <https://doi.org/10.1023/A:1012109513643>.
- [14] S. Furukawa, G. Hattori, S. Sakai, N. Kamiya, Highly efficient and low toxic skin penetrants composed of amino acid ionic liquids, *RSC Adv.* 6 (2016) 87753–87755, <https://doi.org/10.1039/C6RA16926K>.
- [15] R. Ferraz, L.C. Branco, C. Prudêncio, J.P. Noronha, Ž. Petrovski, Ionic liquids as active pharmaceutical ingredients, *ChemMedChem* 6 (2011) 975–985, <https://doi.org/10.1002/cmdc.201100082>.
- [16] J.L. Shamshina, R.D. Rogers, Overcoming the problems of solid state drug formulations with ionic liquids, *Ther. Deliv.* 5 (2014) 489–491, <https://doi.org/10.4155/tde.14.28>.
- [17] Z. Yan, L. Ma, S. Shen, J. Li, Studies on the interactions of some small biomolecules with antibacterial drug benzethonium chloride and its active pharmaceutical ingredient ionic liquid (API-IL) benzethonium L-proline at varying temperatures, *J. Mol. Liq.* 255 (2018) 530–540, <https://doi.org/10.1016/j.molliq.2018.02.007>.
- [18] M. Shadid, G. Gurau, J.L. Shamshina, B.-C. Chuang, S. Hailu, E. Guan, S.K. Chowdhury, J.-T. Wu, S.A.A. Rizvi, R.J. Griffin, R.D. Rogers, Sulfasalazine in ionic liquid form with improved solubility and exposure, *Med. Chem. Commun.* 6 (2015) 1837–1841, <https://doi.org/10.1039/C5MD00290G>.
- [19] H. Yoshiura, M. Tamura, M. Aso, N. Kamiya, M. Goto, Ionic liquid-in-oil microemulsions as potential carriers for the transdermal delivery of methotrexate, *J. Chem. Eng. Jpn.* 46 (2013) 794–796, <https://doi.org/10.1252/jcej.13we009>.
- [20] M. Moniruzzaman, N. Kamiya, M. Goto, Ionic liquid based microemulsion with pharmaceutically accepted components: formulation and potential applications, *J. Colloid Interface Sci.* 352 (2010) 136–142, <https://doi.org/10.1016/j.jcis.2010.08.035>.
- [21] C.M. Raihan, R.M. Moshikur, R. Wakabayashi, Y. Tahara, N. Kamiya, M. Moniruzzaman, M. Goto, Ionic-liquid-based paclitaxel preparation: a new potential formulation for cancer treatment, *Mol. Pharm.* 15 (2018) 2484–2488, <https://doi.org/10.1021/acs.molpharmaceut.8b00305>.
- [22] O. Zavgorodnya, J.L. Shamshina, M. Mittenenthal, P.D. McCrary, G.P. Rachiero, H.M. Titi, R.D. Rogers, Polyethylene glycol derivatization of the non-active ion in active pharmaceutical ingredient ionic liquids enhances transdermal delivery, *New J. Chem.* 41 (2017) 1499–1508, <https://doi.org/10.1039/C6NJ03709G>.
- [23] K. Mioduszewska, J. Dołżonek, D. Wyrzykowski, Ł. Kubik, P. Wiczling, C. Sikorska, M. Toński, Z. Kaczyński, P. Stepnowski, A. Białk-Bielińska, Overview of experimental and computational methods for the determination of the pKa values of 5-fluorouracil, cyclophosphamide, ifosfamide, imatinib and methotrexate, *TrAC Trends Anal. Chem.* 97 (2017) 283–296, <https://doi.org/10.1016/j.trac.2017.09.009>.
- [24] Y. Ohta, Y. Kondo, K. Kawada, T. Teranaka, N. Yoshino, Synthesis and antibacterial activity of quaternary ammonium salt-type antibacterial agents with a phosphate group, *J. Oleo Sci.* 57 (2008) 445–452, <https://doi.org/10.5650/jos.57.445>.
- [25] A. Foulet, O. Ben Ghanem, M. El-Harbawi, J.M. Lévêque, M.I.A. Mutalib, C.Y. Yin, Understanding the physical properties, toxicities and anti-microbial activities of choline-amino acid-based salts: low-toxic variants of ionic liquids, *J. Mol. Liq.* 221 (2016) 133–138, <https://doi.org/10.1016/j.molliq.2016.05.046>.
- [26] A. Yazdani, M. Sivapragasam, J.M. Leveque, M. Moniruzzaman, Microbial biocompatibility and biodegradability of choline-amino acid based ionic liquids, *J. Microb. Biochem. Technol.* 08 (2016) 415–421, <https://doi.org/10.4172/1948-5948.1000318>.
- [27] S. Wu, L. Zeng, C. Wang, Y. Yang, W. Zhou, F. Li, Z. Tan, Assessment of the cytotoxicity of ionic liquids on *Spodoptera frugiperda* 9 (SF-9) cell lines via in vitro assays, *J. Hazard. Mater.* 348 (2018) 1–9, <https://doi.org/10.1016/j.jhazmat.2018.01.028>.
- [28] A.A. Elgharbawy, F.A. Riyadi, M.Z. Alam, M. Moniruzzaman, Ionic liquids as a potential solvent for lipase-catalysed reactions: a review, *J. Mol. Liq.* 251 (2018) 150–166, <https://doi.org/10.1016/j.molliq.2017.12.050>.
- [29] L. Yu, Amorphous pharmaceutical solids preparation, characterization, *Adv. Drug Deliv. Rev.* 48 (2001) 27–42, [https://doi.org/10.1016/S0169-409X\(01\)00098-9](https://doi.org/10.1016/S0169-409X(01)00098-9).
- [30] Z. Wojnarowska, J. Knapik, M. Rams-Baron, A. Jedrzejowska, M. Paczkowska, A. Krause, J. Cielecka-Piontek, M. Jaworska, P. Lodowski, M. Paluch, Amorphous protic ionic systems as promising active pharmaceutical ingredients: the case of the sumatriptan succinate drug, *Mol. Pharm.* 13 (2016) 1111–1122, <https://doi.org/10.1021/acs.molpharmaceut.5b00911>.
- [31] C. Agatemor, K.N. Ibsen, E.E.L. Tanner, S. Mitragotri, Ionic liquids for addressing unmet needs in healthcare, *Bioeng. Transl. Med.* (2018) 7–25, <https://doi.org/10.1002/btm2.10083>.
- [32] M. Dhanka, C. Shetty, R. Srivastava, Methotrexate loaded gellan gum microparticles for drug delivery, *Int. J. Biol. Macromol.* 110 (2018) 346–356, <https://doi.org/10.1016/j.ijbiomac.2017.12.026>.
- [33] X. Han, W. Qi, W. Dong, M. Guo, P. Ma, J. Wang, Preparation, optimization and in vitro-in vivo investigation for capsules of the choline salt of febuxostat, *Asian J. Pharm. Sci.* 11 (2016) 715–721, <https://doi.org/10.1016/j.ajps.2016.05.009>.
- [34] R. Liu, N. Sadrzadeh, P.P. Constantinides, in: R. Liu (Ed.), *Water-Insoluble Drug Formulation*, Interpharm Press, Denver, CO, 2000.